

# **Thermography of flame during diesel fuel combustion with steam gasification**

I.S. Anufriev<sup>1</sup>, M.V. Agafontsev<sup>2</sup>, E.P. Kopyev, E.L. Loboda<sup>2</sup>,  
O.V. Sharypov<sup>1</sup>

<sup>1</sup>Institute of Thermophysics SB RAS, Novosibirsk, 630090,  
Russia

<sup>2</sup>Tomsk State University, Tomsk, 634050, Russia

e-mail: [kopyev.evgeniy@mail.ru](mailto:kopyev.evgeniy@mail.ru)

*The paper represents a study concerning the combustion of liquid hydrocarbon fuel in a perspective burner device with the controlled forced supply of overheated steam into the combustion zone, using diesel fuel. The thermal imaging measurements are conducted for the outer flame of the burner device in the wide range of regime parameters (flow rate and temperature of steam). A thermal imaging camera (FLIR, JADE J530SB) is used in the experiments. The effective emissivity coefficient of flame is obtained versus the flow rate of steam supplied. The steam*

*parameters are found to influence on the temperature in the outer flame of the burner device.*

## **1 Introduction**

Fuel gasification is the conversion of solid or liquid fuel into combustible gases by using the partial oxidation during the high temperature heating [1, 2]. The gasification of organic fuels is used in some cases for processing of low grade fuels to produce a synthesis gas [3]. The synthesis gas obtained is used as a final product for manufacturing purposes, for example as gaseous fuels for thermal electric power stations or as a hydrogen source (for example, the production of ammonia), carbon black, etc. [4-8]. In addition, this gaseous fuel releases a smaller amount of toxic gases during combustion compared to original fuel. Steam is often used as an oxidizer for fuel gasification and the synthesis gas produced is called a water gas.

Also, steam is used as a sprayer in fuel nozzles [9]. This improves the solubilizing of black oil and intensifies its vaporization and combustion. There are the other examples of

using steam during the fuel combustion, for example, the supply of steam into the combustion chamber of a gas turbine installation allows the content of toxic nitrogen oxides to be reduced in combustion products due to decreasing the flame temperature [10, 11].

In addition, the injection of water or steam into the combustion chambers of thermal electric power stations (using liquid or solid fuel) is also used to reduce NO<sub>x</sub> emissions. There are the examples of the water injection into the internal-combustion engines in automobiles, in order to suppress detonation, decrease carbonization and reduce NO<sub>x</sub> and CO concentrations [12, 13]. In all these applications, water (steam) acts as a cooling component used to dilute a fuel mixture, which allows the temperature and the formation of thermal NO<sub>x</sub> to be reduced in the combustion zone. However, this method leads to the decrease in the power and efficiency of equipment, and its use is limited since CO emissions and other products of incomplete fuel combustion start increasing along with the reduction of NO<sub>x</sub>. Therefore, the use of steam during the fuel

combustion in a certain device requires a comprehensive scientific evidence to select the optimal (according to environmental and thermotechnical specifications) modes and structural parameters.

At the Institute of Thermophysics SB RAS a new method is proposed for fuel combustion with the use of steam, when there is the gasification of carbon-containing particles during the incomplete combustion of liquid hydrocarbons [14]. The supply of overheated steam to the liquid hydrocarbon combustion zone was shown to sharply intensify combustion [15, 16]. This provides stable ignition, high completeness of fuel combustion and a low content of toxic components in combustion products. This method of combustion is promising for utilization of low-grade liquid hydrocarbon fuels and combustible industrial wastes to produce heat energy. In the previous papers [15-17] the authors used an autonomous burner device with constant steam parameters (flow rate and temperature) [18, 19]. However, these characteristics should be adjusted to control the combustion process. In this work a new burner device equipped with an

electric steam generator is used to obtain a flow of overheated steam for the wide range of flow rates and temperatures. To study the effect of steam parameters on the main characteristics of the liquid hydrocarbons combustion process (the composition of combustion products and the specific heat release capacity), it is necessary to obtain the data for different combustion modes.

This paper represents the thermal imaging study concerning the flame of a perspective burner device during the combustion of diesel fuel along with the supply of overheated steam to the combustion zone for the wide range of steam parameters.

## **2 Experimental setup and measurement procedure**

The studies were conducted using a firing stand (Fig.1) equipped with a new burner device (10 kW), an electric steam generator (average power of 1.5 kW), a plunger metering pump, an automatic steam generator control system, a fuel supply system, an electronic balance to control the flow of water and fuel, as well as with necessary control and measurement instruments. The main elements of the new burner device are: a cylindrical body, a

combustion chamber, a steam nozzle and a gas-generation chamber. The combustion chamber has holes for the air inflow from the atmosphere. Fuel is supplied into the combustion chamber through the fuel pipe. The stable rate of fuel is provided by the fuel nozzle and the pump and controlled by the electronic balance. A steam nozzle is mounted coaxially above the combustion chamber near the base of the gas-generation chamber and is oriented vertically (outlet diameter is 0.5 mm). The steam nozzle is connected with an external steam generator. The test burner is a vaporizing burner according to the operation principle. The combustion process is similar to the operation of an autonomous burner [17].

The steam generator consists of three heating units connected in sequence. Each unit is a metal tube (38 mm in external diameter) with a length of 0.5 m and a wall thickness of 8 mm. An electric tubular U-shaped heater (maximum power of 700 W) was mounted inside the pipe. The space between the heater and the pipe wall was filled with periclase DM-1 to increase heat transfer. In the wall of each pipe there are the

closed rectangular cross-section channels (4×2 mm and 6 m in length for each block) in the form of spiral. The pipes are insulated outside. The monitoring temperature sensors are installed on the surface of each block. The mass flow of water (steam) is provided by the plunger metering pump and controlled by the electronic balance. The steam temperature is regulated by changing the power of the heaters. The pressure in the steam generator is recorded by the digital pressure sensor. The developed laboratory electric steam generator produces the overheated steam in the range of the temperature and flow rate of 100÷600°C and 0.25÷1.5 kg/h (pressure up to 10 atm).

The thermal imaging camera (FLIR, JADE J530SB) was used to measure the temperature in the high temperature flame of the burner device. This device has a high temporal resolution: the frame rate up to 177 Hz with a maximum resolution of 320x240 pixels and up to 18 kHz with a resolution of 320x4 pixels. The minimum time of frame exposure is 6 μs. The operating range of the thermal imager is in the middle infrared range of 2.5-5.0 microns. The same spectral range contains the powerful flame

radiation lines caused by the radiation of hot combustion products (including water vapors, CO<sub>2</sub>, and CO). Based on the results of previous studies [20], a narrow spectral band dispersion optical filter F0616 with bandwidth of 2.5-2.7 microns was selected for operation.

The filter was selected due to the powerful emission lines of water vapors and CO<sub>2</sub> in this spectral range. The temperature measurement range of the thermal imager is determined by calibration and reaches 583-1773 K for the filter selected. The data collection and initial processing of thermograms were carried out using a specialized program, Altair. The factory calibrations were used for the F0616 filter with an exposure time of 9, 64, and 350  $\mu$ s for the operation of the thermal imager. The previous spectral analysis of the flame temperature and pressure [20] demonstrated the absence of peak periodic oscillations in the test flame. To obtain an average temperature value, the measurements were conducted with a frequency of 50 Hz for 1 min.



To determine the effective emissivity coefficient simultaneously with the thermal imager measurements at the control points (on the axis of the burner device  $r = 0$ , at the height  $x = 30$  mm from the edge of the burner), the temperature was recorded using a platinum-platinum rhodium type B thermocouple (600...1600°C) with the thermoelectrodes 300 microns in diameter. The thermal inertia of the thermal converter was not more than 5 seconds. The permitted deviation limits of thermoelectromotive forces were  $\pm 0.005$  compared with the standard static characteristics of the converter for the value of the measured temperature. Using the thermogram, the average temperature was determined in the area of hot junction. The effective emissivity coefficient, the values of which were ranged from 0.3 to 0.65 depending on the steam flow, was selected using the Altair software. The value of the effective emissivity coefficient obtained was used for the entire area.

### **3 Measurement results and analysis**

Measurements were carried out under different operating conditions of the burner device. For the constant rate of fuel  $F_f = 0.82$  kg/h, the value  $\gamma = F_v / (F_v + F_f)$  was varied in the range of  $0.24 \div 0.56$ , where  $F_v$  is the average mass flow rate of steam. The steam temperature was varied in the range of  $T_v = 160 \div 560^\circ\text{C}$  for each value of  $F_v$ .

Fig. 2 shows the time-average temperature profiles in the outer flame of the burner device for different flow rates of steam at  $T_v = \text{const}$ . It should be noted that the flame is a translucent three-dimensional optical medium, so the thermal imager detects the integral radiation of all inner medium layers. This integral radiation is required to determine the temperature in the observation plane, using the calibrations and the effective emissivity coefficient. The thermograms shown on Fig. 2 demonstrate a significant effect of the supplied steam flow both on the temperature distribution in the outer flame and the flame dimensions (photographs in Fig. 2).

Fig. 3 shows the flame temperature versus the height at the different flow rates and temperatures of steam supplied. ( $\gamma = 0.56$ ).

The analysis of the results shows (Fig. 3a), that the maximum flame temperature ( $T_{\max}$ ) is achieved at a maximum flow rate of steam ( $\gamma = 0.56$ ). At the same time, a longitudinal size of the luminous area is minimal (photograph in Fig. 2d). (The experiments showed that a further increase in the  $\gamma$  parameter led to the blowout of flame, and a low flow rate of steam ( $\gamma < 0.3$ ) led to the incomplete combustion of fuel). The maximum flame temperature increases with the increase in the steam temperature (Fig. 3b).

For the modes with a high value of the parameter  $\gamma$  the height dependence of the flame temperature is monotonous, and the maximum is reached at the outlet of the burner. When  $\gamma \leq 0.5$  the maximum temperature is observed at some distance from the outlet of the burner, which indicates the incomplete mixture combustion before the release into the atmosphere.

The emissivity coefficient of flame  $\varepsilon$  was determined versus the flow rate of the steam supplied (Fig. 4): the value  $\varepsilon$  decreases with increasing the  $\gamma$  parameter. The  $\gamma$  parameter dependence of

the maximum flame temperature is also linear, but increases with increasing  $\gamma$  (Fig. 4).

The experimental data obtained can be used for the measurement analysis of the gas composition in combustion products and the heat release, in order to provide a scientific evidence for the selection of the energy-efficient and environmentally friendly utilization ways for off-grade liquid hydrocarbons to produce thermal energy.

Research was supported by the Russian Science Foundation (Project No. 17-79-20209).

## References

- [1] C. Higman, M. Van Der Burgt, *Gasification. (2<sup>nd</sup> ed.)* (Gulf Professional Publishing, 2008)
- [2] N.V. Lavrov, A.P. Shurygin, *Introduction to the theory of fuel combustion and gasification* (Acad. Sciences of the USSR, Moscow, 1962) – in Russian

- [3] J. Rostrup-Nielsen, L.J. Christiansen, *Concepts in Syngas Manufacture (Catalytic Science Series. Vol. 10)* (Imperial College Press, London, 2011)
- [4] K. Liu, Ch. Song, V. Subramani, *Hydrogen and Syngas Production and Purification Technologies* (John Wiley & Sons, Inc., Hoboken, New Jersey, 2010)
- [5] J. Rezaiyan, N. Cheremisinoff, *Gasification Technologies: A Primer for Engineers and Scientists* (Taylor & Francis, 2005)
- [6] Emanuele Graciosa Pereira, Jadir Nogueira da Silva, Jofran L. de Oliveira, Cssio S. Machado, *Renewable and Sustainable Energy Reviews* **16**, 4753 (2012)
- [7] I.I. Ryabtsev, A.E. Volkov, *Gas production from liquid fuels for synthesis of ammonia and alcohols* (Khimiya, Moscow, 1968) – in Russian
- [8] F.A. Andreev, S.I. Kargin, L.I. Kozlov, V.F. Pristavko, *Combined nitrogen technology* (Khimiya, Moscow, 1974) – in Russian
- [9] D.M. Khzmlyan, J.A. Kagan, *Combustion theory and furnace arrangements* (Energia, Moscow, 1976) – in Russian

- [10] S.V. Tsanev, V.D. Burov, A.N. Remezov, *Gas turbine and steam-gas plants of thermal power stations* (MEI, Moscow, 2002) – in Russian
- [11] A.A. Ivanov, A.N. Ermakov, R.A. Shlyakhov, *Izv. RAN. Energetika* **3** 119 (2010) – in Russian
- [12] M.O. Lerner, *Khimia i zhizn'* **5** 16 (1981) – in Russian
- [13] P.K. Efremov, Proceedings of the All-Union Scientific Conference «Protection of air pool from pollution by toxic emissions vehicles» **1** 93 (1977) – in Russian
- [14] M.S. Vigriyanov, V.V. Salomatov, S.V. Alekseenko, Russian Federation Patent No. 2219435 (2003) – in Russian
- [15] S.V. Alekseenko, S.E. Pashchenko, V.V. Salomatov, *J. Engng. Physics and Thermophysics* **83** 729 (2010)
- [16] S.V. Alekseenko, I.S. Anufriev, M.S. Vigriyanov, V.M. Dulin, E.P. Kopyev, O.V. Sharypov, *Thermophysics and Aeromechanics* **3** 393 (2014)
- [17] S.V. Alekseenko, I.S. Anufriev, M.S. Vigriyanov, E.P. Kopyev, O.V. Sharypov, *Combustion, Explosion, and Shock Waves* **52** 286 (2016)

- [18] M.S. Vigriyanov, S.V. Alekseenko, I.S. Anufriev, O.V. Sharypov Russian Federation Patent No. 2523591 (2014) – in Russian
- [19] M.S. Vigriyanov, S.V. Alekseenko, I.S. Anufriev, O.V. Sharypov Russian Federation Patent 2579298 (2016) – in Russian
- [20] I.S. Anufriev, E.P. Kopyev, E.L. Loboda, Proc. SPIE 9292 «20<sup>th</sup> International Symposium on Atmospheric and Ocean Optics: Atmospheric Physics», 929226 (2014)

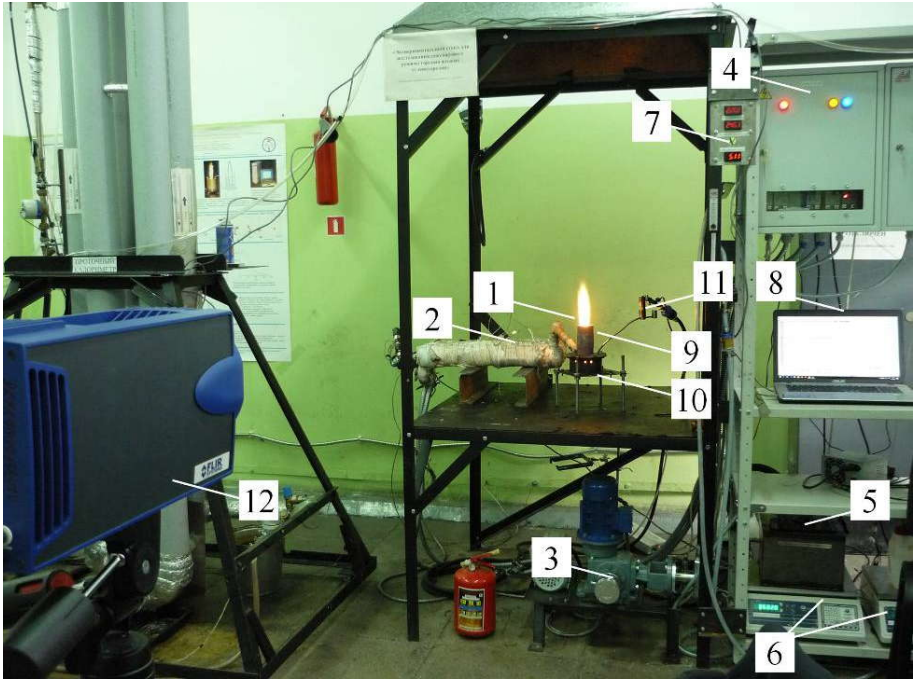


Figure 1. Anufriev I.S. « Thermography of flame during diesel fuel combustion with steam gasification »



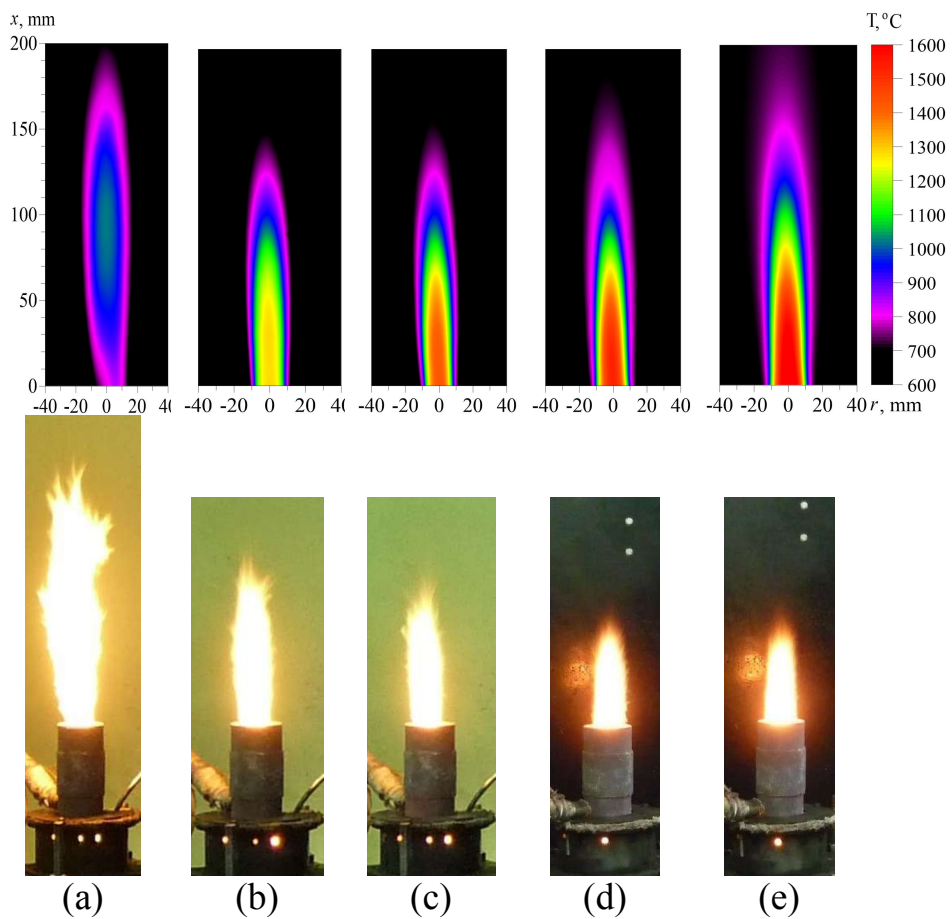
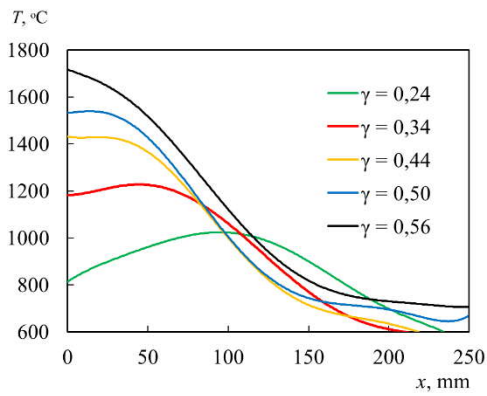
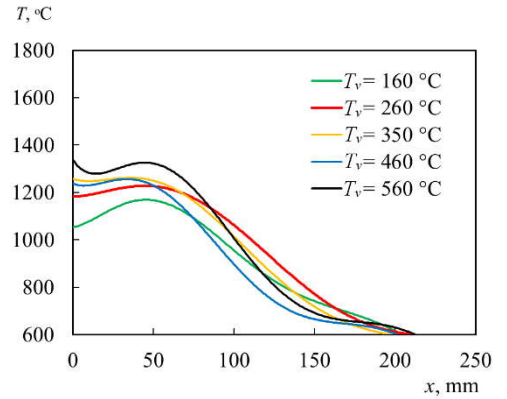


Figure 2. Anufriev I.S. « Thermography of flame during diesel fuel combustion with steam gasification »



(a)



(b)

Figure 3. Anufriev I.S. « Thermography of flame during diesel fuel combustion with steam gasification »

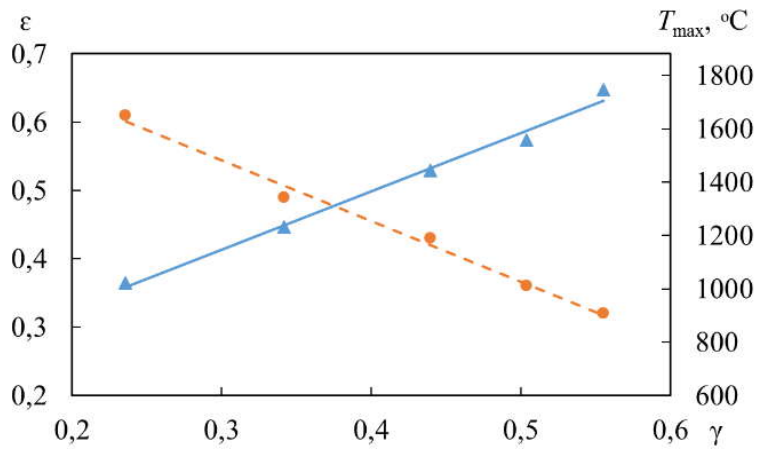


Figure 4. Anufriev I.S. « Thermography of flame during diesel fuel combustion with steam gasification »

**Fig. 1.** Firing stand for the study of liquid hydrocarbon combustion with steam gasification: 1 is the burner device, 2 is the electric steam generator, 3 is the plunger metering pump, 4 is the automatic steam generator control system, 5 is the fuel supply system, 6 is the electronic balance, 7 is the indicators of control and measurement instruments, 8 is the computer, 9 is the gas-generation chamber of the furnace unit, 10 is the combustion chamber of the furnace unit, 11 is the fuel pipe, 12 is the thermal imager

**Fig. 2.** Thermograms of flame and the photographs for different steam flow rates (at a constant temperature steam  $T_v \sim 250$  °C:  $\gamma = 0.24$  (a),  $\gamma = 0.34$  (b),  $\gamma = 0.44$  (c),  $\gamma = 0.50$  (d),  $\gamma = 0.56$  (e), and a steam pressure in the range of  $8 \div 2$  atm, respectively.

**Fig. 3.** Distribution of the time-average temperature in the outer flame along the vertical center line of the flame for different mode parameters: (a) the steam flow rate is varied,  $T_v = 250$  °C; (b) the steam temperature is varied,  $\gamma = 0.34$ , the steam pressure is 4 atm.

**Fig. 4.** Effective emissivity coefficient of flame (●) and maximum temperature (▲) in the outer flame versus the  $\gamma$  parameter,  $T_v=250$  °C